Int. J. Heat Mass Transfer. Vol. 25, No. 4, pp. 487 497, 1982
Printed in Great Britain

0017 9310/82/040487 11 $03.00/0

AN EXPERIMENTAL AND THEORETICAL STUDY OF GAS BUBBLE DRIVEN CIRCULATION SYSTEMS

J. H. GREVET, J. SZEKELY and N. EL-KADDAH
Department of Materials Science and Engineering, Massachusetts Institute of Technology, Cambridge, MA 02139, U.S.A.

(*Received* 27 *January* 1981 *and in revised form* 13 *July* 1981)

Abstract—Experimental measurements are reported on the velocity fields and the turbulence parameters in a cylindrical tank, containing water, which is being agitated by a gas bubble stream, introduced axisymmetrically.

The experimental measurements were compared with theoretical predictions, based on the k–ε model. It was found that predictions and measurements agreed very well regarding the time-smoothed velocity fields, but the agreement was less good (but still satisfactory) regarding the turbulence characteristics of the system.

The measurements have shown that the turbulence was largely isotropic in the bulk of the fluid, furthermore no significant damping of turbulence was observed near the free surface.

NOMENCLATURE

- A, cross-section area of 2-phase region [m^2];
- g, acceleration due to gravity [m/s^2];
- H, height of the liquid column [m];
- k, turbulent kinetic energy [$(m/s)^2$];
- P, pressure [$kg/m.s^2$];
- P', modified pressure, $P - \rho gz$ [$kg/m\ s^2$];
- Q, volumetric flow rate [m^3/s];
- r, radial coordinate [m];
- r_c, radius of 2-phase region [m];
- R, radius of the bath [m];
- U, mean velocity [m/s];
- U', r.m.s. velocity;
- U_{∞}, rising velocity of a single bubble [m/s];
- z, axial coordinate [m];
- $\bar{\alpha}$, average void fraction of the gas in the 2-phase region;
- ε, turbulent energy dissipation [m^2/s^3];
- μ, viscosity [kg/m.s];
- ν, kinematic viscosity [m^2/s];
- ρ, density [kg/m^3];
- λ, jet cone angle.

Subscripts

- eff, effective;
- g, gas;
- l, liquid;
- o, orifice;
- r, radial direction;
- t, turbulent;
- z, axial direction;
- θ, tangential direction.

1. INTRODUCTION

THERE are numerous physical systems of industrial importance, where a melt or liquid phase, contained in a cylindrical vessel is being agitated by an ascending gas bubble stream. Various effluent purification systems and a large number of pyrometallurgical operations may be cited as examples [1–4]. While in most of these systems the ultimate objective is to effect a chemical change in the liquid phase, knowledge of the fluid flow phenomena has to be a key component of any effort aimed at providing a good quantitative representation of these systems.

During the past decade a considerable effort has been made to develop a quantitative representation of these systems in terms of various models of turbulent recirculating flows [5–8]. The experimental verification of these models has been somewhat more problematic.

In general one may state that the overall fields that may be generated by agitating a fluid contained in a cylindrical vessel, by an axisymmetrically introduced gas jet or gas bubble stream may be adequately represented by using a variety of turbulence models [9]. It should be noted that the principal mechanism of momentum transfer in these systems is thought to be associated with convection, rather than with the diffusive transport mechanism; it follows that the predictions regarding the velocity fields are not expected to be very sensitive to the particular turbulence model chosen.

However, if we were to consider these systems as reactors, then the knowledge of the turbulence characteristics of the system (such as the Reynolds stresses, the turbulent energy dissipation and the like) is thought to be of crucial importance because of its role in determining the rates of various processes which may occur in these systems.

As an example, the rate of turbulent energy dissipation will have a major effect in determining the mass transfer coefficient between the fluid and suspended solid particles [10, 11]; furthermore the turbulent energy dissipation will also play a key role in determining the agglomeration rates of suspended solids [12, 13]. Furthermore, the turbulence levels in the system should have a significant effect in determining mass transfer rates between the fluid and the walls, and

hence affecting the erosion rates of the walls in case of high temperature melts.

In contrast to the reasonable level of understanding developed regarding the gross features of the circulation, our knowledge of the turbulence characteristics is much less complete. A necessary prerequisite of developing such information is the need to generate careful measurements of these quantities and then to develop appropriate interpretation for these measurements.

The purpose of the work, which will be described in this paper, is part of an ongoing effort aimed at generating such an improved understanding, with the ultimate objective of applying the results to the interpretation of certain metals processing operations.

2. APPARATUS AND EXPERIMENTAL PROCEDURE

2.1. *Apparatus*

The apparatus was constructed so as to allow the convenient measurement of the velocity fields and the turbulence characteristics in a cylindrical tank containing water, which is being agitated by an ascending gas bubble stream.

A schematic sketch of the tank is shown in Fig. 1. It is noted that the cylindrical inner tank was enclosed in a larger, rectangular container, in order to minimize the parallaxis effects.

A schematic outline of the apparatus as a whole is shown in Fig. 2, where it is seen that the measurement of the velocities and of the turbulence characteristics was accomplished through the use of a laser anemometer. A TSI Laser anemometer was used, employing a Spectrophysics No. 124, He–Ne laser. The anemometer was operated in a dual beam mode, with the analysis of the forward scattered light. The key operating parameters of the system are summarized in Table 1.

2.2. *Experimental procedure*

A typical experimental run involved filling the cylindrical vessel to a predetermined level with distilled water. Proper seeding was provided by adding approximately 40 p.p.m. of powdered milk as indicated in [14]. Then the air was turned on to provide a predetermined linear velocity at the nozzle. Once steady state conditions had been attained, measurements were made of the mean velocity (components), the r.m.s. velocity (components) and the Reynolds stresses.

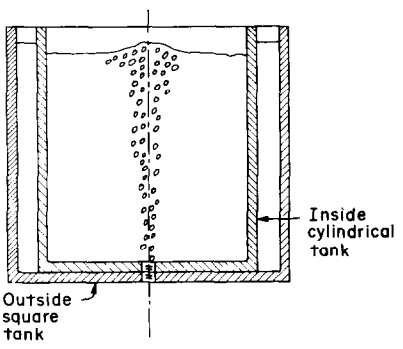

FIG. 1. Schematic diagram of the apparatus.

An interesting feature of the present investigation was that measurements were made not only of the axial (U_z) and the radial (U_r) velocity components but that data have also been obtained on the tangential velocity component (U_θ). Further experimental details are available in the thesis upon which this work is based [15].

The velocity measurements involved the use of essentially standard procedures commonly employed in laser anemometry. The Reynolds stresses were obtained by taking measurements regarding a certain direction and then displacing these by 45° following the relation:

$$\overline{U_i'U_j'} = \frac{1}{2}[U_1'^2 - U_2'^2]$$

where $U_1'^2$ and $U_2'^2$ are the fluctuating velocities at $+45°$ and $-45°$ from the coordinates i and j.

The procedure for obtaining Reynolds stresses by such means is again well documented [16].

3. THE THEORETICAL MODEL

In essence the gas bubble driven circulation system represents an axisymmetrical turbulent recirculating flow problem of the type which has been tackled by numerous investigators. One of the main problems encountered in previous investigations was to obtain a proper representation of the boundary between the gas bubble-rich jet cone region and the bulk of the liquid, both in terms of position and in terms of stating the proper boundary conditions for the velocity and the velocity gradients.

In the present work we followed the standard computational procedures for such systems, but with the following exceptions:

(1) The whole domain was represented in terms of a single set of equations.

(2) The buoyancy forces, which drive the flow were represented by calculating an axially variable density deficit, in the plume, the dimensions of which were determined experimentally. Thus the governing equations used were of the following form:

equation of continuity:

$$\frac{1}{r}\frac{\partial}{\partial r}(\rho r U_r) + \frac{\partial}{\partial z}(\rho U_z) = 0; \tag{1}$$

momentum balance in the z-direction:

$$\frac{1}{r}\frac{\partial}{\partial r}(\rho r U_r U_z) + \frac{\partial}{\partial z}(\rho U_z^2) = -\frac{\partial p'}{\partial z} + \frac{1}{r}\frac{\partial}{\partial r}\left[r\mu_{\text{eff}}\frac{\partial U_z}{\partial r}\right] \tag{2}$$

$$+ 2\frac{\partial}{\partial z}\left[\mu_{\text{eff}}\frac{\partial U_z}{\partial z}\right] + \frac{1}{r}\frac{\partial}{\partial r}\left(\mu_{\text{eff}} r\frac{\partial U_r}{\partial r}\right) + \rho g\bar{\alpha};$$

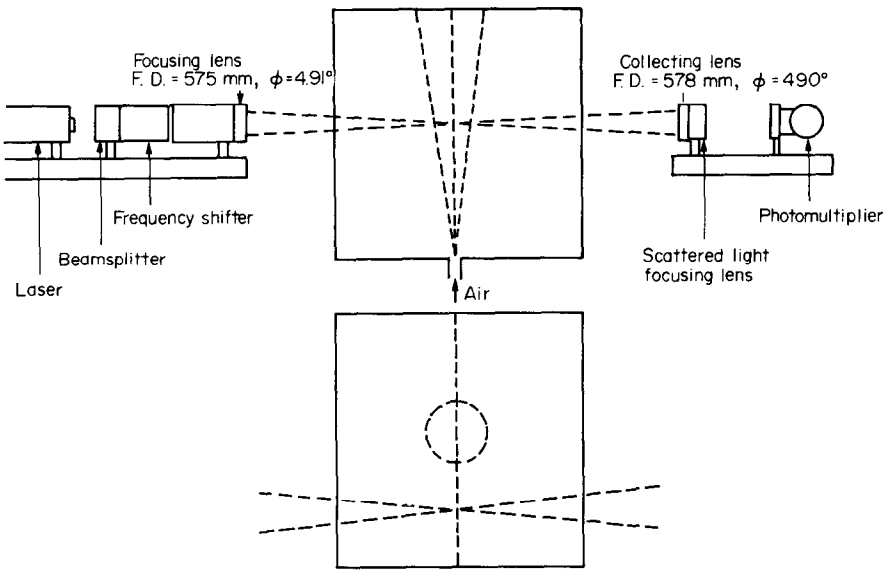

FIG. 2. Sketch of the apparatus, also showing the laser anemometer assembly.

Table 1. Key operating parameters

System parameters for the water model	
Diameter of vessel	0.60 m
Height of water	0.60 m
Orifice diameter	0.127 m (0.5 in)
Velocity of air at nozzle	1.62 m/s and 3.20 m/s
Characteristics of laser and optical arrangements	
Type	Spectra-Physics Model 124—He–Ne
Power	15 MV
Wavelength	6328 Å
Optical arrangement	Dual-beam with forward scatter

momentum balance in the r-direction:

$$\frac{1}{r}\frac{\partial}{\partial r}(\rho r U_r^2) + \frac{\partial}{\partial z}(\rho U_r U_z) = -\frac{\partial p'}{\partial r} + \frac{2}{r}\frac{\partial}{\partial r}\left[r\mu_{\text{eff}}\frac{\partial U_r}{\partial r}\right] + \frac{\partial}{\partial z}\left[\mu_{\text{eff}}\frac{\partial U_r}{\partial z}\right] + \frac{\partial}{\partial z}\left[\mu_{\text{eff}}\frac{\partial U_z}{\partial z}\right] - \frac{2U_r\mu_{\text{eff}}}{r^2}, \quad (3)$$

where

$$\rho = \rho_l,\ r > r_c, \quad (4)$$

$$\rho = \bar{\alpha}\,\rho_g + (1-\bar{\alpha})\,\rho_l,\ r < r_c. \quad (5)$$

It follows that for the purpose of modelling the whole domain has been treated as a homogenous medium, but with a spatially variable density. Using drift flux model which allows the slip between the bubbles and the fluid, the quantity $\bar{\alpha}$ may be expressed as [17]:

$$\bar{\alpha} = \frac{1}{2\pi}\frac{Q_g - \pi r_c^2\,\bar{\alpha}(1-\bar{\alpha})U_\infty}{\int_0^r r U_z dr}, \quad (6)$$

where U_∞ is the rising velocity of a characteristic single bubble, which is estimated as 40 cm/s [18].

The boundary conditions were given as:

at the axis

$$U_r = 0;\ r = 0, \quad (7)$$

$$\frac{\partial U_z}{\partial r} = 0;\ r = 0, \quad (8)$$

at the walls

$$U_r = U_z = 0, \quad (9)$$

at the free surface

$$U_z = 0;\ z = H, \quad (10)$$

$$\frac{\partial U_r}{\partial z} = 0;\ z = H, \quad (11)$$

at the orifice

$$U_z = U_0;\ r = 0,\ z = 0. \quad (12)$$

The governing equations were solved numerically, retaining the primitive variables, and using the well

known k–ε model for the turbulent viscosity (Appendix 1). A 12 × 20 grid was used and the computational procedure was similar to that described by Spalding *et al.* [19]. A selection of the computed results will be given in a subsequent section where these will be compared with the measurements.

4. EXPERIMENTAL MEASUREMENTS AND COMPUTED RESULTS

In this section we shall present a selection of the experimental measurements and these will be compared with the computed values of the corresponding parameters. The material to be presented will include information on the velocities, on the turbulent kinetic energy and on the Reynolds stresses.

4.1. *The mean velocity field*

Figure 3(a, b) show a comparison between the experimentally measured and the theoretically predicted velocity fields; Figs. 4(a, b) show a similar comparison but for a larger nozzle velocity.

It is seen that the agreement between measurements and predictions is reasonably good. It should be noted that the use of k–ε model, in conjuction with appropriate wall functions will give a significantly better agreement between the measurements and the predictions, especially in the near wall regions than would the use of simpler computational procedures, employing a single value of the effective viscosity [8].

A more critical test of the model is to compare the predictions regarding the radial dependence of the absolute value of the velocity vector with the measurements.

This is done in Figs. 5(a–f) using a greatly expanded scale. It is seen that the agreement is quite reasonable throughout the domain, with the exception of the region near the bottom of the vessel and near the jet boundary. Regarding the latter it is not quite clear at this stage whether the discrepancy is attributable to any shortcomings of the model or to the possible errors in the measurements, which were quite difficult to make in the vicinity of the jet boundary.

Figure 6 shows the computed velocity distribution in the jet cone region, which has been normalized with respect to the maximum (centerline) velocity. It is seen that this normalized axial velocity is essentially independent of the axial position. The Gaussian type distribution found seems to be in good agreement with the experimental measurements of Tse-Chang *et al.* [20].

It is noted that measurements were also made of U_θ which were found to be close to zero in all cases. However, as will be shown subsequently $U_\theta'^2 \neq 0$.

4.2. *Turbulence characteristics of the system*

Figure 7(a, b) show the profiles of the r.m.s. velocity components normalized with respect to the mean velocity in the jet cone at the corresponding vertical position. A somewhat simplified analytical method was used for estimating the latter quantity (Appendix 2).

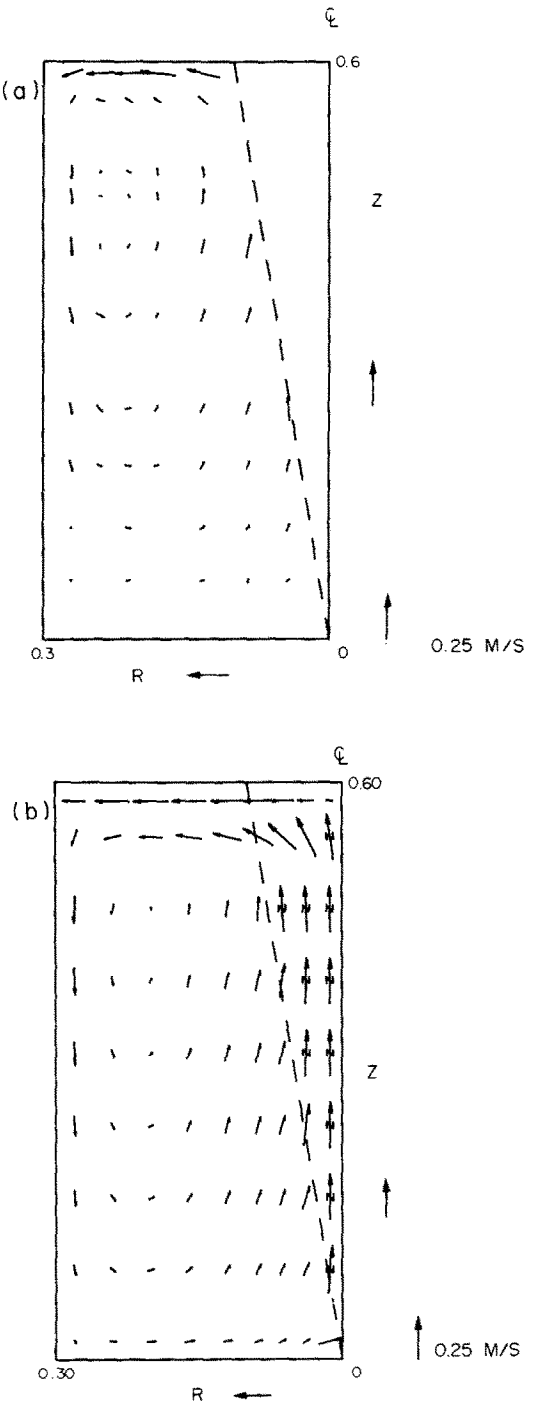

FIG. 3. A comparison of the experimentally measured and the computed velocity profiles for a linear gas velocity of 1.6 m/s at the orifice. (a) Experimental measurements, (b) theoretical predictions.

Inspection of Fig. 7 allows two interesting deductions to be made: one of these is that the turbulence appears to be farily isotropic, except in the vicinity of the solid surfaces (side walls or the bottom), which is essentially in line with expectations.

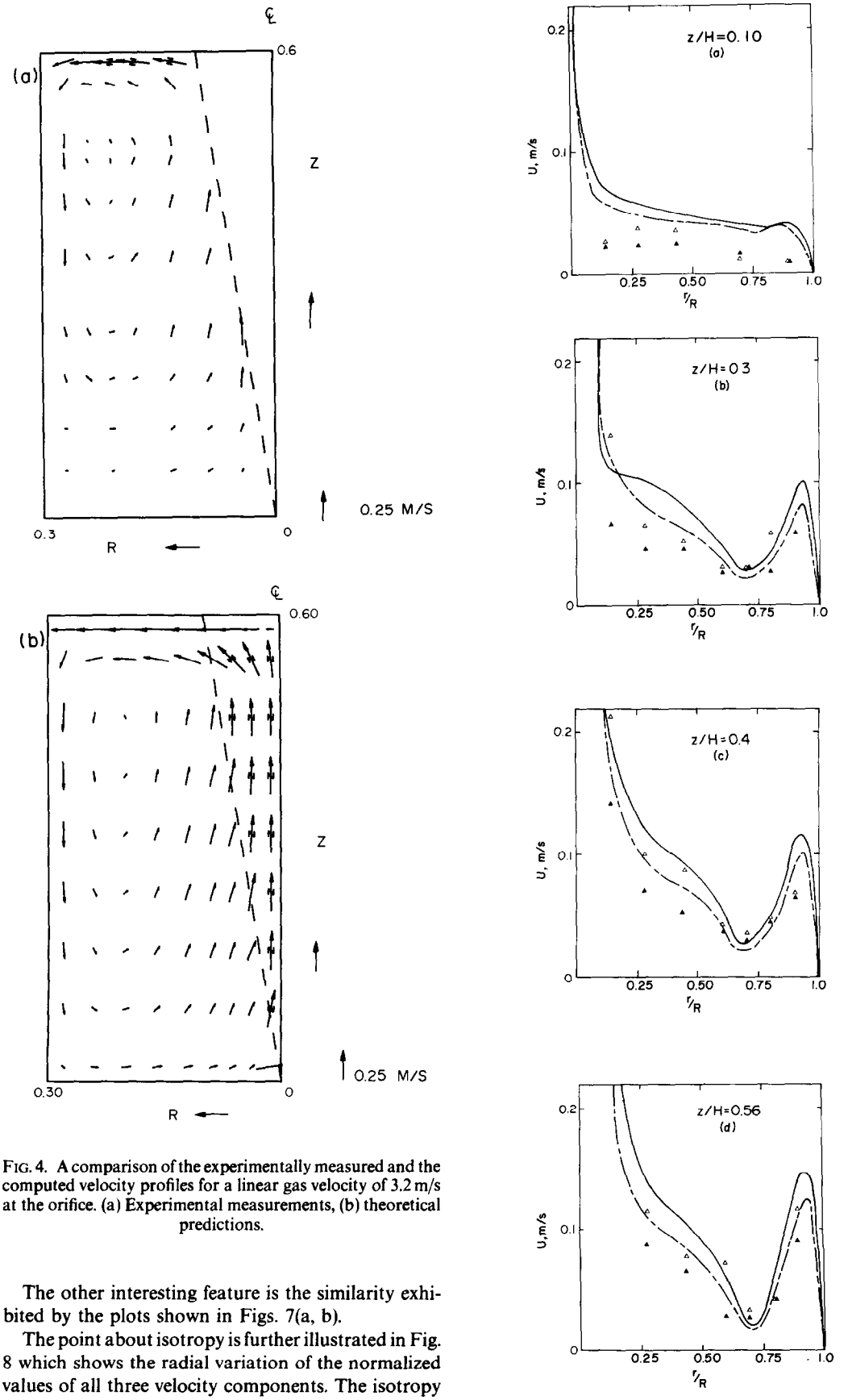

FIG. 4. A comparison of the experimentally measured and the computed velocity profiles for a linear gas velocity of 3.2 m/s at the orifice. (a) Experimental measurements, (b) theoretical predictions.

The other interesting feature is the similarity exhibited by the plots shown in Figs. 7(a, b).

The point about isotropy is further illustrated in Fig. 8 which shows the radial variation of the normalized values of all three velocity components. The isotropy exhibited by these results in the bulk of the fluid

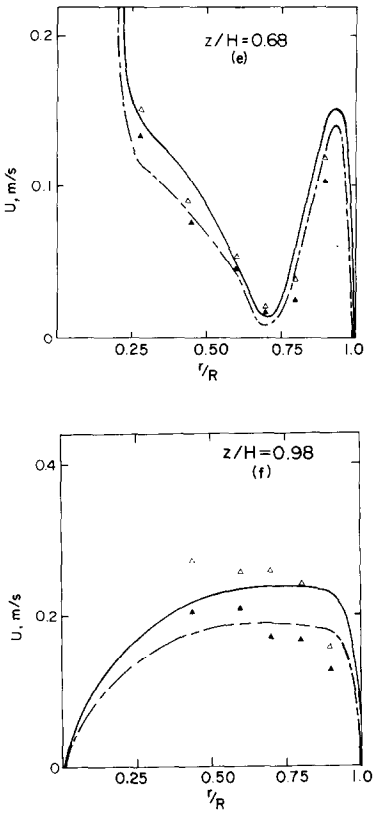

FIG. 5. The radial dependence of the absolute value of the velocity vector—a comparison of the predictions with measurements at various axial positions. (a) Experimental measurements for an orifice velocity of 162 cm/s (▲) and 320 cm/s (△), (b) theoretical predictions for an orifice velocity of 162 cm/s (– · —) and 320 cm/s (——).

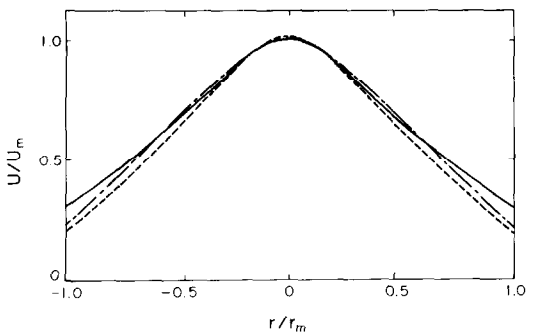

FIG. 6. The predicted radial variation of the normal velocity in the jet cone region for various axial positions: z/H = 0.85 cm (——), z = 0.60 cm (— — — —), and z = 0.33 cm (—— · ——).

provides *a posteriori* justification for the assumption made by many investigators in the calculation of the turbulent kinetic energy.

Figures 9(a–e) show a comparison between the experimentally measured and the calculated values of the turbulent kinetic energy. The agreement seems to be within about a factor of two in most cases, which is

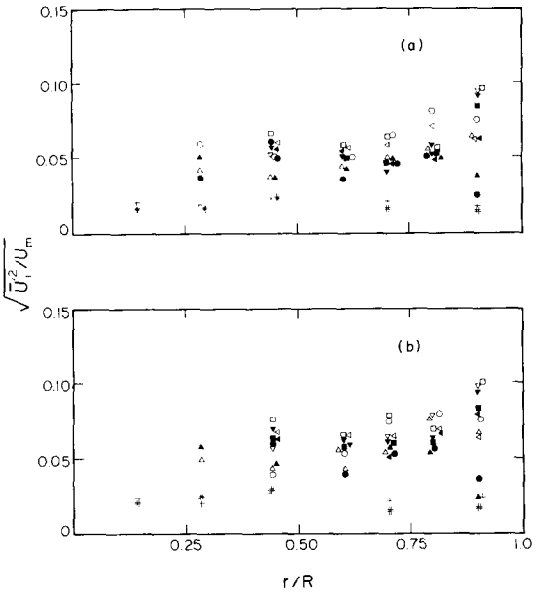

FIG. 7. The experimentally determined, normalized radial profile of the r.m.s. velocity components. (a) Linear orifice velocity 1.62 m/s, (b) linear orifice velocity 3.20 m/s. Notation: $\sqrt{U_z'^2}$ and $\sqrt{U_r'^2}$ for z/H = 0.81 (▽, ▼); 0.68 (□, ■); 0.56 (▽ ▼); 0.40 (○, ●); 0.30 (△, ▲); 0.10 (+, #).

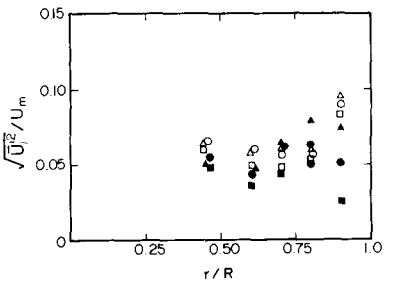

FIG. 8. The radial variation of the r.m.s. velocity components for an orifice velocity of 1.62 m/s – U_z'/U_{2j}, U_r'/U_{zj} U_θ'/U_{zj} for z/H = 0.68 (△, □, ○) and 40 (▲, ■, ●).

not unreasonable; but this discrepancy indicates that further study, of these phenomena would be fully justified. This further theoretical work could involve either the adjustment of the parameters in the k–ε model or perhaps the development of an alternative modelling approach.

It should be noted that the turbulent kinetic energy has much higher value at the free surface than in the bulk. This behaviour underlines the fact that Levich's ideas of turbulence damping by surface tension forces would be inappropriate for such highly turbulent fluid flows. Similar suggestions have been made by other investigators [21, 22].

This finding does of course, have very important implications regarding mass transfer phenomena.

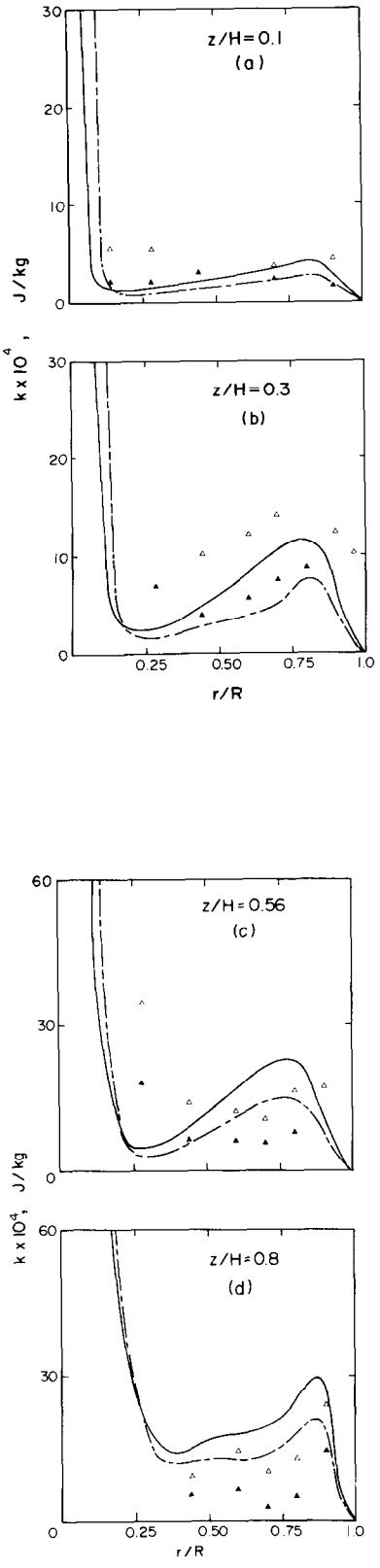

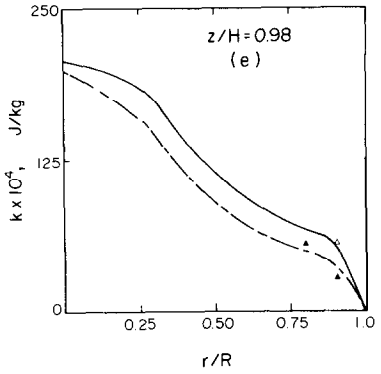

FIG. 9. The radial variation of the turbulent kinetic energy — a comparison of the measurements with predictions at various axial positions. Experimental measurements for an orifice velocity of 162 cm/s (▲) and 320 cm/s (△). Experimental measurements for an orifice velocity of 162 cm/s (— — —) and 320 cm/s (———).

4.3. *Reynolds stresses*

The current mathematical models employed in the computational approaches toward turbulent recirculating flows all rely on suitable postulates regarding the behavior of the Reynolds stresses. For this reason it is of interest to examine the Reynolds stresses explicitly.

This is done in Tables 2 and 3 showing a comparison between the experimentally measured and the theoretically predicted values of the Reynolds stresses. It is seen that the results are in semiquantitative agreement, but that quite substantial discrepancies exist at particular locations.

One should remark here, as was done in case of the turbulent kinetic energy that a further refinement of the k–ε model would be desirable.

Finally Figs. 10(a, b) show the computed contours of the turbulent viscosity for two gas flow rates. It is seen that this ratio is quite high. Furthermore quite substantial variations exist in the turbulent viscosity so that the use of a single, constant value is unlikely to be satisfactory, except as a first approximation.

5. DISCUSSION

Extensive experimental measurements have been carried out to determine the velocities and the turbulence characteristics in a cylindrical vessel, containing water, which was being agitated by an axially introduced air bubble stream. The experimental measurements were compared with theoretical predictions, which were based on the k–ε model, written for the entire domain. The actual buoyancy driven flow was represented by assigning an appropriate, axially variable density deficit to the jet cone, the boundaries of which were determined experimentally.

In considering the results of the present investigation the following principal points may be made:

Table 2. Measured and calculated Reynolds stresses $\rho \overline{U_r' U_z'}$, for 1.62 m/s

Z/H	r/R 0.90	0.80	0.70	0.60	0.44	0.28	0.14
(1)	−0.9	−7.2	−6.2	−3.2	−3.4		
0.98						—	—
(2)	−11.1	−16.3	−9.7	−5.2	+1.7		
(1)	+1.6	+0.8	−2.6	−2.7	+2.5		
0.93						—	—
(2)	−3.4	−6.9	−5.6	−4.8	−2.7		
(1)	+5.0	+1.3	+0.5	+0.5	+2.3		
0.77						—	—
(2)	+3.0	+3.3	+1.7	+0.3	−0.2		
(1)	+3.7	+2.2	+0.6	+0.2	+0.9	+10.8	
0.68							
(2)	+3.0	+4.7	+3.7	+2.3	+0.8	+1.4	
(1)	+0.3		+0.8	+1.1	+0.6	+0.4	+0.6
0.19							
(2)	+0.5		+0.7	+0.5	+0.2	+0.1	+0.9

1, measured; 2, computed.

Table 3. Measured and calculated Reynolds stresses $\rho \overline{U_r' U_z'}$ for 3.2 m/s

Z/H	r/R 0.90	0.80	0.70	0.60	0.44	0.28	0.14
(1)	+6.3	−7.5	−11.4	−8.4	−3.6		
0.98							
(2)	−12.7	−25.1	−15.2	−8.6	+0.9		
(1)	+2.3	+2.5	−7.8	−4.1	+8.7		
0.93						—	—
(2)	−5.7	−10.7	−8.9	−7.7	−4.4		
(1)	+9.9	+3.0	+1.1	+1.1	+0.1		
0.77						—	—
(2)	+4.7	+5.4	+2.9	+0.5	−0.3		
(1)	+1.5	+4.1	+1.0	+0.3	+2.8	+44.4	
0.68							—
(2)	+4.9	+7.7	+6.1	+3.8	+1.3	+1.4	
(1)	+1.0		+3.8	+1.4	+2.2	+1.7	−0.9
0.19							
(2)	+0.8		+1.1	+0.8	+0.3	+0.2	+0.6

1, measured; 2, computed.

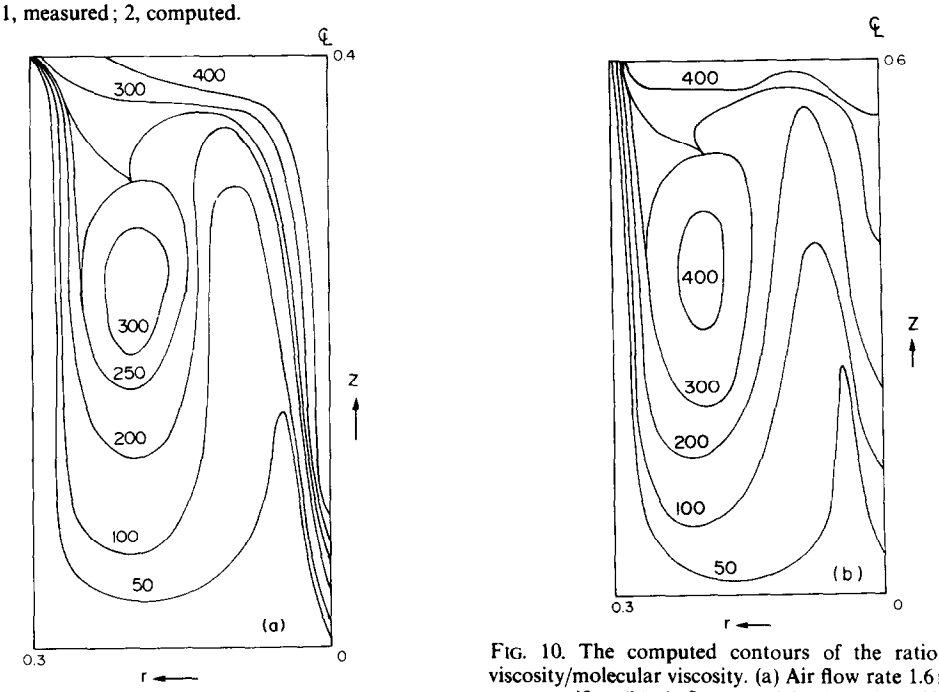

FIG. 10. The computed contours of the ratio: effective viscosity/molecular viscosity. (a) Air flow rate 1.6 m/s at the orifice, (b) air flow rate 3.2 m/s at the orifice.

(1) The theoretically determined and the experimental measured velocity profiles were found to be in good agreement. It should be noted, however that since the principal mechanism of momentum transfer in these systems is due to convection, one may expect fairly good agreement between the measured and the predicted velocities, even if the effective viscosity is not very well represented.

(2) The agreement between the experimentally measured and the theoretically predicted turbulence energies and Reynolds stresses was rather less satisfactory, although these values were usually within about a factor of two. This would suggest that further work would be desirable regarding possible refinements of the $k-\varepsilon$ model.

It should be noted that the magnitude of these discrepancies is rather similar to those reported in an earlier paper [23] describing turbulent recirculating flow in a belt driven system. Under those conditions there were fewer ambiguities associated with the definition of the boundary conditions in the central portion of the vessel. It would appear therefore that these discrepancies may well be associated with the incorrect selection of the constants, or perhaps with the inherent shortcomings of the $k-\varepsilon$ model for representing systems of this type. Clearly the development of an additional experimental data base for the critical assessment of the $k-\varepsilon$ model for representing turbulent recirculating in liquids would be highly desirable.

Other, perhaps lesser reasons for the discrepancy may be associated with the model proposed for the jet cone region, which postulated no radial variations in the void fraction.

(3) The experimental measurements have shown that the turbulent fluctuations were largerly isotropic in the bulk of the fluid, a finding which provides *a posteriori* justification for the expressions used in the calculation of the turbulent kinetic energy. Marked anisotropy was, however found in the vicinity of the walls, which is to be expected.

(4) Inspection of the maps of the turbulent energy of the system has shown that the turbulent kinetic energy is relatively uniform in the bulk of the fluid; however one has found markedly higher values of the turbulent kinetic energy in the vicinity of the jet cone and near the surface, while the turbulent kinetic energy was rather lower near the bottom surface.

This behavior has interesting implications regarding the use of gas bubble stirred systems as reactors or contacting devices.

It is quite possible that in many of these systems the various kinetic processes, such as desulfurization, agglomeration of fine particles, etc. occur predominately in the regions of high turbulence. Under these conditions the overall rate limiting step may be the rate at which reactants are being transported into these active zones, rather than the factors that govern the absolute levels of turbulence or turbulent energy dissipation rates in the regions. The consideration of these factors could well lead to an improved design of these installations [24].

Acknowledgements—The authors wish to thank the National Science Foundation for partial support of this investigation under Grant No. DMR78-24692-MCS.

REFERENCES

1. W. G. Wilson and A. McLean, Desulfurization of iron and steel and sulfide shape control, *Iron and Steel Soc. A.I.M.E.*, (1980).
2. Scaniject, I. *Proc. Int. Conf. Injection Metallurgy, MEFOS, Lulea, Sweden* (1977).
3. Scaniject II, *Proc. Int. Conf. Injection Metallurgy, FOS, Lulea, Sweden* (1980).
4. J. S. Kirkaldy, *McMaster Symposium on Ladle Treatment of Carbon Steel, Hamilton, Canada* (1970).
5. J. Szekely, H. Y. Wang and K. M. Kiser, Flow Pattern Velocity and Turbulence Energy Measutements and Predictions in a Water Model of an Argon-Stirred Ladle, *Met Trans.* **7B**, 287–295 (1976).
6. T. DebRoy, A. K. Majundar and D. B. Spalding, Numerical Prediction of Recirculation Flows with Free Convection Encountered in Gas-Agitated Reactor. *Appl. Math. Modelling* **2**, 146–150 (1978).
7. J. W. McKelliget, M. Cross, R. D. Gibson and J. K. Brimacombe, Mathematical Modelling of Submerged Gas Jets, *I.C.H.M.T. Int. Sem. on Heat and Mass Transfer in Met. Systems*, Dubrovnik, Yugoslavia (Sept. 1979).
8. J. Szekely, N. H. El-Kaddah and J. Grevet, Flow Phenomena in Argon-Stirred Ladles, Room Temperature Measurements and Analysis, *Int. Conf. Injection Metallurgy, Lulea, Sweden*, 5:1–5:32 (1980).
9. B. E. Launder and D. B. Spalding, *Mathematical Models of Turbulence*. Academic Press (1972).
10. R. Shinnar and J. M. Church. Statistical Theories of Turbulence in Predicting Partial Size in Agitated Dispersions, *Ind. Engng Chem.* **52**, 253–256 (1960).
11. S. Middleman, Mass. Transfer from Particles in Agitated Systems Application of the Kolmogoroff Theory, *A.I.Ch.E. Jl.* **11**, 750–752 (1965).
12. P. G. Saffman and J. S. Turner, On The Collision of Drops in Turbulent Clouds, *J. Fluid Mech.* **1**, 16–30 (1956).
13. V. G. Levich, *Physicochemical Hydrodynamics*. Prentice Hall (1962).
14. W. K. George and J. L. Lumley, The Laser Doppler Velocimeter and Its Application to the Measurements of Turbulence, *J. Fluid Flow Mech.* **60**, 321–362 (1973).
15. J. Grevet, MSc. Thesis, MIT (Jan. 1981).
16. TSI, *LDA Instruction Manual*.
17. G. B. Wallis, *One dimensiomal Two-Phase Flow*. McGraw Hill (1969).
18. R. Clift, J. R. Grace and M. G. Weber, *Bubbles, Drops and Particles*. Academic Press, New York (1978).
19. W. M. Pun and D. B. Spalding, A General Computer Program for Two-Dimensional Elliptic Flows, Report HTS 76/2 Heat Transfer Section, Imperial College, London (1977).
20. H. Tse-Chang, T. Lehner and B. Kiellberg, Fluid Flow in Ladles—Experimental Results, *Scand. J. Met.* **9**, 105–110 (1980).
21. M. Kh. Kishinevsky, Two Approaches to the Theoretical Analysis of adsorption Processes, *J. appl. Chem. U.S.S.R.* **28**, 881–886 (1955).
22. M. Kh. Kishinevsky and V. T. Serebryunsky, The Mechanism of Mass Transfer at the Gas Liquid Interface, *J. appl. Chem. U.S.S.R.* **29**, 29–33 (1957).

23. J. Szekely, A. H. Dilawari and R. Metz, The Mathematical and Physical Modelling of Turbulent Recirculating Flows *Met. Trans.* **10B**, 33–41 (1979).
24. N. El-Kaddah and J. Szekely, A Mathematical Model for Desulfurization Kinetics in Argon Stirred Ladle, *Ironmaking and Steelmaking*, **8**, 269–278 (1981).

APPENDIX 1

Outline of the k–ε model

The k–ε model postulates that the turbulent viscosity μ_t is given by the following relationship:

$$\mu_t = C_D \frac{\rho k^2}{\varepsilon},$$

where k is the turbulent kinetic energy of the fluid and ε is the rate of dissipation of the turbulent kinetics energy. C_D is a constant.

The spatial distribution of the quantities k and ε is then obtained, through the solution of conservation equations, which take the following form in the cylindrical coordinate system.

$$\frac{\partial}{\partial z}(\rho U_z \phi) + \frac{1}{r}\frac{\partial}{\partial r}(\rho r U_r \phi) - \frac{\partial}{\partial z}\left(\frac{\mu_{eff}}{\sigma\phi}\right)\frac{\partial \phi}{\partial z}$$

$$-\frac{1}{r}\frac{\partial}{\partial r}\left(r\frac{\mu_{eff}}{\sigma\phi}\frac{\partial \phi}{\partial r}\right) = S\phi,$$

where $S\phi$ is the net rate of generation of turbulent properties per units volume. The source terms S_R and S_ϵ of transport equation of k and ε are given by:

$$S_k = G - D,$$

$$S_\epsilon = C_1\, \varepsilon/R\, G - C_2\, \rho\, \varepsilon^2/K,$$

where

$$G = \mu_t\left\{2\left[\left(\frac{\partial U_z}{\partial z}\right)^2 + \left(\frac{\partial U_r}{\partial r}\right)^2 + \left(\frac{U_r}{r}\right)^2\right] + \left(\partial\frac{U_z}{\partial r} + \partial\frac{U_r}{\partial z}\right)^2\right\},$$

$$D = \rho\varepsilon.$$

It follows that ultimately the solution of the fluid flow problem requires the simultaneous solution of five equations, namely: the continuity; the two components of the equation of motion; the two conservation equations for k–ε. In addition the numerical values generated will also depend upon the values chosen for the constants: C_1, C_2, C_D, σ_k, and σ_ε.

APPENDIX 2

In order to calculate the mean velocity in the 2-phase region a homogeneous flow model was adopted.

A momentum balance over a volume element in the axial direction gives

$$\rho U_2^2 \frac{dA}{dz} + 2\rho A U_2 \frac{dU_2}{dz} = \rho\bar{\alpha} g \frac{1}{3}\left(A + z\frac{dA}{dz}\right). \quad (2.1)$$

For the 2-phase region expanding at an angle λ equation 2.1 becomes

$$\frac{2U_z^2}{z} + 2U_z\frac{dU}{dz} = \bar{\alpha} g. \quad (2.2)$$

The void fraction $\bar{\alpha}$ may be calculated from a mass balance on the gas phase as

$$\bar{\alpha} = Q_{gas}/z^2(\tan\lambda)^2\, U_z. \quad (2.3)$$

From equations 2.2 and 2.3 we obtain the following ordinary differential equation which describes the ascending velocity of the 2-phase region.

$$\frac{dU_z}{dz} + \frac{U_z}{z} = Q_g g/2\ (\tan\lambda)^2\, U_z^2 z^2. \quad (2.4)$$

The boundary conditions are:

$$z = 0,\ U_z = U_o.$$

ETUDE EXPERIMENTALE ET THEORIQUE DE SYSTEMES D'ECOULEMENT PRODUIT PAR UN COURANT DE BULLES GAZEUSES

Résumé—On décrit des mesures expérimentales sur le champ de vitesse et les paramètres de turbulence dans un réservoir cylindrique qui contient de l'eau agitée par un courant axisymétrique de bulles gazeuses.

Les mesures sont comparées aux calculs basés sur le modèle k–ε. On trouve que les calculs et les mesures s'accordent très bien en ce qui concerne les champs de vitesse moyens dans le temps, mais l'accord est moins satisfaisant (quoique acceptable) relativement aux caractéristiques de la turbulence dans le système.

Les mesures montrent que la turbulence est largement isotrope dans le coeur du fluide et que la turbulence n'est pas amortie près de la surface libre.

EINE EXPERIMENTELLE UND THEORETISCHE STUDIE VON ZIRKULATIONS SYSTEMEN DIE VON GASBLASEN ANGETRIEBEN WERDEN

Zusammenfassung—Es wird über Messungen des Geschwindigkeitsfeldes und der Turbulenzparameter in einem zylindrischen Tank berichtet, dessen Wasserinhalt von einem achsensymmetrisch eingeführten Gasblasenstrom aufgerührt wird.

Die Meßergebnisse wurden mit theoretischen Berechnungen auf der Grundlage des k–ε–Modells verglichen. Es zeigte sich, daß Rechnungen und Experimente bezüglich der zeitlich geglätteten Geschwindigkeitsfelder gut übereinstimmten, während die Übereinstimmung im Hinblick auf die Turbulenzparameter des Systems weniger gut (aber immer noch zufriedenstellend) war. Die Messungen zeigten, daß die Turbulenz im größten Teil der Flüssigkeit praktisch isotrop war. An der freien Oberfläche wurde keine nennenswerte Dämpfung der Turbulenz beobachtet.

ЭКСПЕРИМЕНТАЛЬНОЕ И ТЕОРЕТИЧЕСКОЕ ИССЛЕДОВАНИЕ ТЕЧЕНИЙ, ВЫЗВАННЫХ ДВИЖЕНИЕМ ГАЗОВЫХ ПУЗЫРЬКОВ

Аннотация — Представлены результаты измерения полей скорости и параметров турбулентности в цилиндрическом сосуде, заполненном водой, приводимой в движение осесимметричной струей газа, вдуваемого в жидкость. Данные экспериментальных измерений сравниваются с результатами расчета по модели $k - \varepsilon$. Найдено, что для осредненных по времени полей скорости результаты расчетов хорошо согласуются с измеренными значениями. Что касается характеристик турбулентности, то совпадение оказывается менее хорошим, но все же удовлетворительным. Измерения показали, что турбулентность является в основном изотропной во всем объеме жидкости и, кроме того, почти незатухающей у свободной поверхности.